Kinetic structure of a two-dimensional liquid

M. M. Hurley and Peter Harrowell
Department of Physical and Theoretical Chemistry, University of Sydney, Sydney, New South Wales 2006, Australia
(Received 27 February 1995)

On an intermediate time scale, a molecular dynamics simulation of a two-dimensional (2D) liquid of soft disks exhibits dramatic structural and kinetic inhomogeneities. We introduce a local relaxation time (defined as the time required for a particle to first travel a distance r from its initial position) in order to present a quantitative analysis of this kinetic structure. The length r is chosen so as to maximize the resolution of the kinetic structure. This analysis produces a natural measure of cooperativity. We demonstrate that caging in the 2D liquid takes place in a subset of particles only, distributed as transient clusters throughout the liquid.

PACS number(s): 61.20.Ja, 61.20.Lc, 66.10.−x

I. INTRODUCTION

A simple two-dimensional (2D) liquid exhibits striking transient correlations involving both local structure and kinetics. Consider the plot of particle trajectories in Fig. 1 collected over a time interval in which each particle undergoes approximately 20 collisions during a molecular dynamics (MD) simulation of a 2D liquid of soft disks. (The details are described below.) Particles are clearly segregated spatially into those undergoing oscillatory motion within hexagonally ordered clusters and those exhibiting an enhanced mobility about the edges of these clusters. This behavior has been noted often in the extensive literature on 2D liquids, having been seen in analog [1] and computer [2] simulations and in studies of confined colloidal suspensions using photon correlation of light scattering [3] and microscopy [4]. At the densities and temperature of the simulation shown in Fig. 1, this structure (including orientational "hexatic" correlations) vanishes with long time averaging, leaving us with an isotropic liquid. Although hidden in long time averages, the transient inhomogeneities would be expected to play an important role in phenomena that probe the liquid at intermediate frequencies. In this paper we present a quantitative analysis of this transient structure of the particle dynamics in a 2D liquid and its relationship with the time-dependent diffusion constant. In the process, we develop a set of general tools for analyzing such transient structure in any simulated liquid or glass.

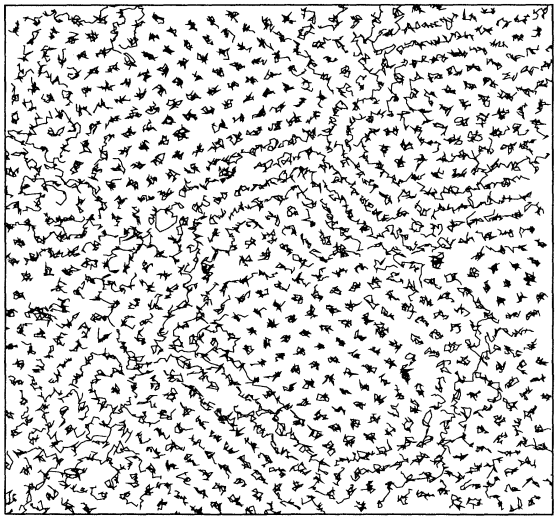

FIG. 1. Trajectories of 780 soft disks at $\rho^*=0.98$ collected over approximately 20 collision times.

To begin we note that the particles depicted in Fig. 1 are distinguished from one another by two features. The first is local structure as measured by the local hexagonal order. The second characteristic is a kinetic one, indicated in Fig. 1 by the distance each particle manages to move within the time interval the trajectories were recorded. These two aspects are obviously intimately linked in the 2D liquid. In this paper we focus on the spatial distribution of the second of these features, the kinetic structure. While the less accessible of the two, we argue that this structure is of more general utility. We may not always know the measure of local structure relevant to collective kinetics but we can always, as described below, determine a local relaxation time and hence a kinetic structure. The spatial distribution of a local relaxation time provides an explicit link between liquid dynamics and the particle fluctuations responsible. This approach has already proved valuable in analyzing the relaxation kinetics in model glass [5] and liquid [6] systems.

II. SIMULATION DETAILS

We have performed a series of MD simulations on a 2D system of 780 soft disks. These particles interact via a repulsive potential $V(r)=\varepsilon(\sigma/r)^{-12}$, which is cut off at a reduced distance ($r^*=r/\sigma$) greater than 2.5 using a shifted potential [7]. Periodic boundary conditions are used. Simulations are done at constant total energy, particle number, and volume. The temperature in reduced units is $T^*=1.00$ (where $T^*=k_BT/\varepsilon$). A reduced time step of $\Delta t^*=0.005$ is used where $\Delta t^*=\Delta t(\varepsilon/m\sigma^2)^{1/2}$ and m is the particle mass. Velocity rescalings were car-

ried out every 4000 time steps in order to correct the numerical creep in total energy without introducing any significant perturbation to the relaxational dynamics of the liquid. The phase diagram for this system has been studied by Broughton, Gilmer, and Weeks [2], who report that, at $T^*=1.00$, the first long-ranged structure appeared at a scaled density of approximately $\rho\sigma^2=\rho^*=0.986$. To ensure that we are studying the dynamics of disordered liquid only, we work at a range of densities from 0.91 to 0.98 and test the pair correlation function $g(r)$ and scattering function for isotropy to confirm that all results refer to phases whose average structure is that of an isotropic liquid.

III. DEFINING A LOCAL RELAXATION TIME

Rather than fix a time interval and record the distribution of particle displacements as done in Fig. 1, it is convenient to define a relaxation time τ of a particle as the length of time taken by that particle to first move a distance r from its initial position. The temporal distribution of particles over the first passage time τ obtained for $r=0.8$ at $\rho^*=0.98$ is shown in Fig. 2. The *spatial* distribution of these relaxation times for a single run can be represented as a map over the simulation cell. In Fig. 3 we compare relaxation time maps from the same run calculated using different values of the cutoff distance r. These maps underline a crucial aspect of the length r. If this distance is too short, then we do not distinguish between the rattling of confined particles and those free to move. The result is a spatial map in which the relaxation times are distributed at random [compare Fig. 3(a) with Fig. 3(b)]. If r is chosen to be so long that each particle will have passed through several domains of fast and slow dynamics before exceeding this distance, we would also find a map of relaxation times with little correlated structure. In this case the length scale of our kinetic criterion would have exceeded that required to resolve the kinetic structures evident in Fig. 1.

What criterion should we use to choose this important length? We argue here that the spatial segregation observed in intermediate time trajectories (as in Fig. 1) is real. We shall therefore choose $r=r_c$ such that the heterogeneity of the kinetic structure is maximized. This choice is simply the value of r optimized to resolve the different types of particle motion, i.e., localized rattling from extended translations. As such, r_c plays a role similar to the transition state of chemical kinetics [8] and constitutes an important length in liquid kinetics.

We now need to quantify the heterogeneity of a spatial distribution of relaxation times. To do this we generate a series of increasingly coarse grained distributions by placing a subcell of dimension $l\times l$ around each particle and assign to the ith particle the mean local relaxation time $\tau_{i,l}$ of the ith cell of size l. The idea is that as we vary the

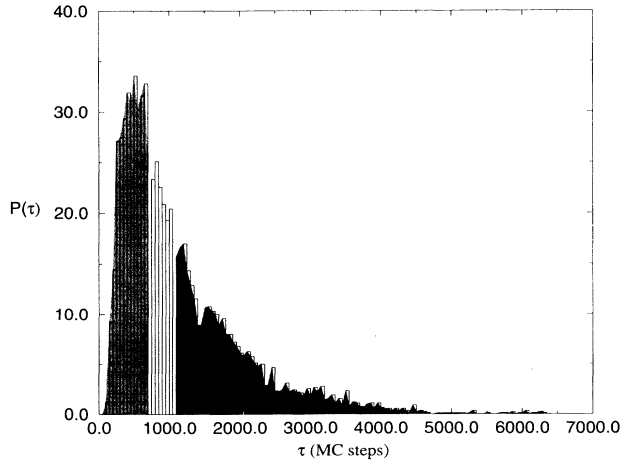

FIG. 2. Distribution $P(\tau)$ of relaxation times at $\rho^*=0.98$. The fastest 40% and the slowest 40% of the particles are indicated by gray and black shadings, respectively.

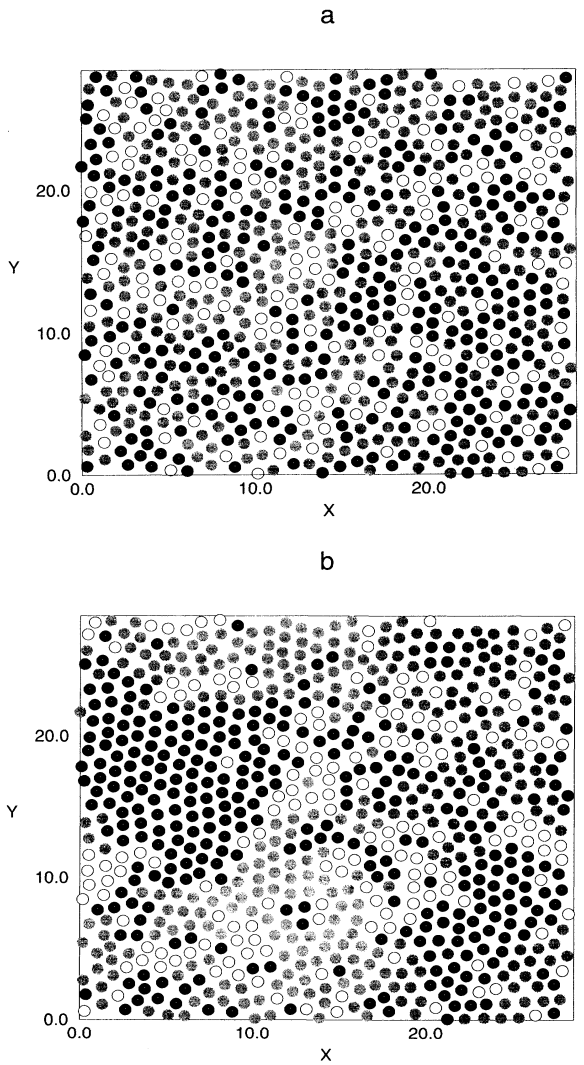

FIG. 3. Maps of the relaxation times of one simulation run at $\rho^*=0.98$ in which the following values of the cutoff distance r are used: (a) $r=0.2$ and (b) $r=0.8$. The circles represent the particle positions at an initial time. The slowest 40% are colored black, the fastest 40% are shaded gray, and the intermediate 20% are unfilled circles. Note the distinct clustering of slow particles seen in (b) but not (a).

subcell dimension l from 1 to L, the system size (and hence the coarseness of our graining), the spatial structure of the relaxation time map disappears. The amount of structure is measured by the second moment $m_2(l)$ of the mean local relaxation time. We define $m_2(l)$ as

$$m_2(l)=\frac{\langle(\tau_{i,l}-\tau_{\rm av})^2\rangle}{\langle(\tau_{i,1}-\tau_{\rm av})^2\rangle}\ , \tag{1}$$

where $\langle\ \rangle$ indicates an average of the subcells indexed by i and $\tau_{i,L}=\tau_{\rm av}$. The values of this function vs l from the simulation of a liquid of density $\rho^*=0.98$ are presented in Fig. 4 for a range of lengths r. Note that a maximum in the decay length of $m_2(l)$ appears to occur for a value of $r\approx 0.8$. This information can be expressed in a characteristic length ξ, calculated as the integral of $m_2(l)$ over l from 1 to L. The larger the extent of clustering of anomalously slow and fast particles, the larger the characteristic length ξ of the decay of $m_2(l)$ with respect to l. It is this quantity that we shall use as our measure of the heterogeneity of the relaxation time distribution. Plots of ξ vs r for three densities are shown in Fig. 5. A number of points of this figure are worth noting. (i) The heterogeneity does in fact exhibit a maximum with respect to the choice of the cutoff length r, just as the qualitative discussion above suggested. (ii) The value of r at this maximum (i.e., r_c) appears to be independent of density (see Table I). (iii) The characteristic length of the kinetic structure at the maximum ξ^* is considerably larger than the length associated with random clumping as given by ξ for $r=0.2$. (iv) The characteristic length is a rapidly increasing function of density (see Table I), consistent with a divergence at the onset of the ordered phase. Note that ξ^* provides an explicit measure of dynamic cooperativity without the need to know the mechanism responsible for relaxation. This feature, we argue, makes the analysis developed here a powerful tool for the general study of cooperativity in liquids and glasses. The existence of these two new lengths r_c and ξ^*, defined in terms of the optimized resolution of the transient kinetic structure of the liquid, make up the first major result of this paper.

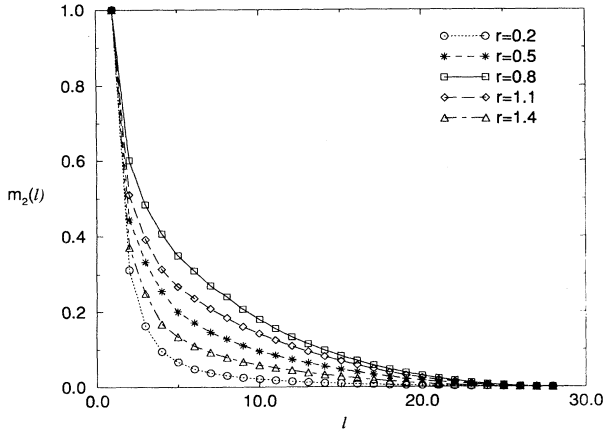

FIG. 4. Second moment $m_2(l)$ of the coarse grained relaxation time distribution plotted against the (reduced) coarse graining length l. Data are presented from relaxation time distributions obtained for five different choices of the cutoff length r. Note the nonmonotonic dependence of the decay length of $m_2(l)$ on r.

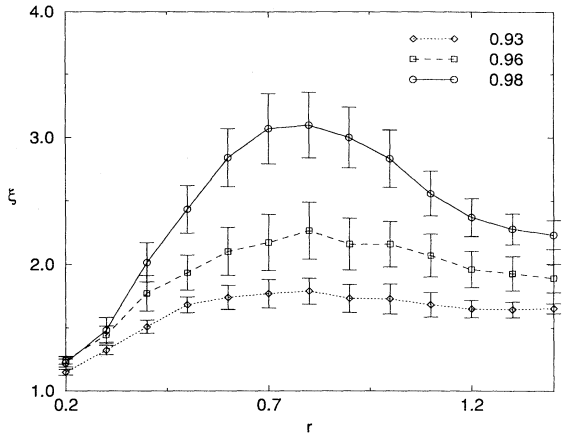

FIG. 5. Characteristic length ξ, calculated as the integral under the curve $m_2(l)$, plotted against the cutoff length r for three densities $\rho^*=0.98$, 0.96, and 0.93. Note the presence of distinct maxima in ξ at each density. The value of r at the maxima r_c is the cutoff length that maximizes the amount of transient structure. Both ξ and r are in reduced units.

IV. RESOLVING CONTRIBUTIONS TO SELF-DIFFUSION

With r_c determined, relaxation times can be assigned to each particle. This allows us to investigate how different subsets of particles, grouped according to their relaxation times, contribute to a transport coefficient, in this case the self-diffusion coefficient. A plot of the mean squared particle displacement vs time (see Fig. 6) is linear except for very short times, an unremarkable result. The value of the diffusion constant, defined here as $d\langle(\Delta r^*)^2\rangle/dt$, is provided in Table I. We now resolve the contribution of this curve into the slowest 40% and the fastest 40% of the particles. Even this crude fractioning presents us, in Fig. 6, with some important results. First, particles retain their identity of "fast" or "slow" for a time period we shall call the mixing time $\tau_{\rm mix}$. This time is defined graphically in Fig. 6 and $\tau_{\rm mix}$ for a range of densities are presented in Table I. If we define a collision time as the time at which the first negative minimum occurs in the velocity autocorrelation function (see below), than at $\rho^*=0.98$, $\tau_{\rm mix}$ is roughly 20 collision times. The extent of this lifetime underlines the stability of the kinetic structure. Second, the distinctive plateau

TABLE I. Density dependence of the diffusion constant D, the mixing time $\tau_{\rm mix}$, and the length scales r_c and ξ^* (all in reduced units).

ρ^*	r_c	D	ξ^*	$\tau_{\rm mix}$
0.98	0.8	0.000 78	3.1	780
0.96	0.8	0.001 01	2.3	680
0.93	0.8	0.001 37	1.8	580

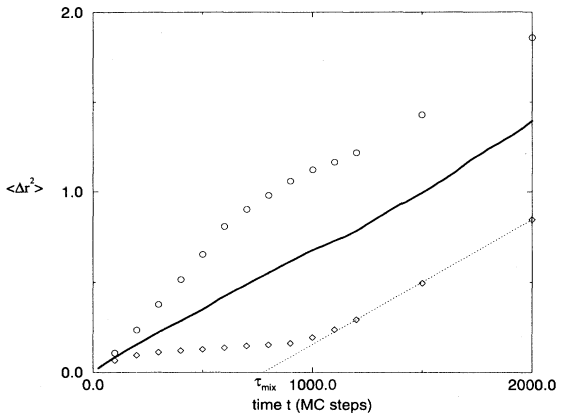

FIG. 6. Mean squared displacement $\langle \Delta r^2 \rangle$ of particles as a function of time at $\rho^* = 0.98$. The total average is indicated by the solid line. The contributions of the fastest 40% (circles) and the slowest 40% (diamonds) of the particles to $\langle \Delta r^2 \rangle$ are identified. The mixing time τ_{mix} is defined as the time intercept of the linear fit to the long time values of $\langle \Delta r^2 \rangle$ of the slow particles.

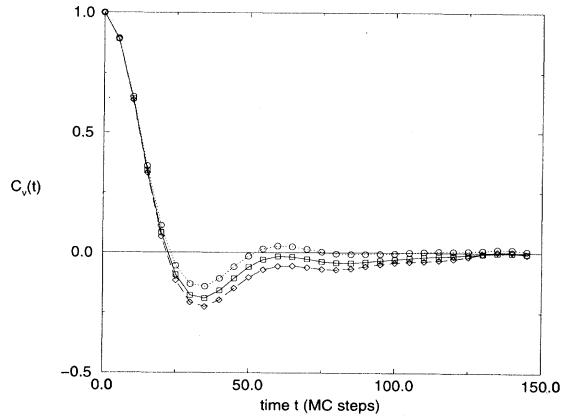

FIG. 7. Velocity autocorrelation function $C_v(t)$ at $\rho^* = 0.98$ is plotted against time. The contributions to the fastest 40% (circles) and the slowest 40% (diamonds) of the particles are identified. Note the distinct negative minimum in the fast component, despite the absence of any evidence of confinement.

in the squared displacement of the slow component is consistent with the physical idea of a transient cage. We consider the implications of this result below. Finally, over the period τ_{mix} the fast fraction exhibits diffusive motion with a diffusion constant that, at $\rho^* = 0.98$, is 1.5 times that of the liquid as a whole. It is not clear whether this enhanced diffusion has its origin in specific dynamic correlations (e.g., the "stringlike" motions reported in earlier studies [1,4]) or in a general density difference between fast and slow domains.

V. SPATIAL CORRELATION OF CAGED PARTICLES

We have demonstrated that slow particles tend to occur in clusters and that caging is restricted to this particle fraction. Together, these results indicate that caging in the 2D liquid is a heterogeneous phenomenon, involving, at any time, only a clustered subset of the liquid particles. [The clustering of the slow particles is easily seen in Fig. 3(b)]. This direct visualization of the spatial distribution of the cage effect through the 2D liquid is the second major result of this paper. We note that the analysis of single-particle dynamics presented here can be immediately extended to 3D liquids. Previous discussions of caging in liquids [9] have regarded the negative values of the velocity autocorrelation function $C_v(t) = \langle [\mathbf{v}_i(0) \cdot \mathbf{v}_i(t)] \rangle / \langle v_i^2 \rangle$ as a signature of confinement. If we look at the contribution of the same slow and fast fractions to $C_v(t)$ in Fig. 7, we find little difference between the two fractions in the first negative region. The significant negative velocity correlation in the fast fraction, which shows no evidence of particle confinement in Fig. 6, suggests that this feature of $C_v(t)$ need have little to do with transient caging.

As the fraction of particles experiencing caging approaches 50%, the overall diffusion constant will be determined by the confinement lifetime τ_{mix}. (Zwanzig [10] has analyzed a simple representation of this situation.) In this simple 2D liquid, however, there is an upper bound on the extent of caging due to the onset of crystallization. Interactions between the hexagonally ordered slow domains ultimately leads to the ordering transition to hexatic or crystal [2]. In a liquid in which the slow domains exist *without* any associated crystalline order, an uninterrupted increase in the extent of such domains (with decreasing temperature or increasing density) becomes possible and would be expected to lead to a glassy state.

VI. CONCLUSION

In conclusion, we have presented a quantitative analysis of the spatial extent of inhomogeneities in the relaxation kinetics of a simple 2D liquid. In the course of this study it has been demonstrated that the optimization of this transient heterogeneity leads naturally to the appearance of two new lengths of importance to the intermediate time scale kinetics of the liquid. These quantities are r_c, the length of the critical fluctuation associated with "cage" escape, and ξ^*, the characteristic linear dimension of the kinetic inhomogeneities. While we may expect for the one-component 2D liquid that ξ^* will scale as the size of the transient hexagonal clusters, there is, in general, no reason for this kinetic correlation length to be simply related to a particular n-body equilibrium correlation length. By way of a counterexample, a range of kinetic lengths are reported in Ref. [5] for the facilitated kinetic Ising model, which (due to the absence of interparticle interactions) has a correlation length of zero for all n-spin equilibrium correlations.

In choosing to address *kinetic* structure, we have

developed an approach that is equally applicable to more complex liquids in three dimensions as it is not tied to any system-specific structural signature. The existence of long-lived populations of slow and fast particles suggest that the van Hove self-correlation function may exhibit a non-Gaussian form over a time interval considerably longer than has been reported in 3D liquids [11]. We are currently examining this point, along with completing a complementary study of the kinetics of the structural fluctuations in the 2D liquid of soft disks.

ACKNOWLEDGMENT

We gratefully acknowledge the support of the Australian Research Council by way of Grant No. A2930072.

[1] B. Pouligny, R. Malzbender, and N. A. Clark, Bull. Am. Phys. Soc. **33**, 436 (1988); A. Stone, G. Warr, and P. Harrowell (unpublished).

[2] J. Q. Boughton, G. H. Gilmer, and J. D. Weeks, Phys. Rev. B **25**, 4651 (1982).

[3] N. A. Clark, B. J. Ackerson, and A. J. Hurd, Phys. Rev. Lett. **50**, 1459 (1983); B. J. Ackerson and N. A. Clark, Faraday Discuss. Chem. Soc. **76**, 219 (1983).

[4] C. A. Murray and R. A. Wenk, Phys. Rev. Lett. **62**, 1643 (1989).

[5] M. Foley and P. Harrowell, J. Chem. Phys. **98**, 5069 (1993); P. Harrowell, Phys. Rev. E **48**, 4359 (1993).

[6] R. Moss and P. Harrowell, J. Chem. Phys. **101**, 9894 (1994).

[7] M. P. Allen and D. J. Tildesley, *Computer Simulations of Liquids* (Oxford University Press, Oxford, 1987), p. 103.

[8] W. Forst, *Theory of Unimolecular Reactions* (Academic, New York, 1973).

[9] A. Gerschel, in *Molecular Liquids—Dynamics and Interactions,* edited by A. J. Barnes (Reidel, New York, 1984), p. 163.

[10] R. Zwanzig, Chem. Phys. Lett. **164**, 639 (1989).

[11] A. Rahman, Phys. Rev. **136**, A405 (1964); W. van Megen and S. M. Underwood, J. Chem. Phys. **88**, 7841 (1988).